
Conditional Matrix Flows for Gaussian Graphical Models

Marcello Massimo Negri

University of Basel

marcellomassimo.negri@unibas.ch

Fabricio Arend Torres

University of Basel

fabricio.arendtorres@unibas.ch

Volker Roth

University of Basel

volker.roth@unibas.ch

Abstract

Studying conditional independence structure among many variables with few observations is a challenging task. Gaussian Graphical Models (GGMs) tackle this problem by encouraging sparsity in the precision matrix through an l_p regularization with $p \leq 1$. However, since the objective is highly non-convex for sub- l_1 pseudo-norms, most approaches rely on the l_1 norm. In this case frequentist approaches allow to elegantly compute the solution path as a function of the shrinkage parameter λ . Instead of optimizing the penalized likelihood, the Bayesian formulation introduces a Laplace prior on the precision matrix. However, posterior inference for different λ values requires repeated runs of expensive Gibbs samplers. We propose a very general framework for variational inference in GGMs that unifies the benefits of frequentist and Bayesian frameworks. Specifically, we propose to approximate the posterior with a matrix-variate Normalizing Flow defined on the space of symmetric positive definite matrices. As a key improvement on previous work, we train a continuum of sparse regression models jointly for all regularization parameters λ and all l_p norms, including non-convex sub- l_1 pseudo-norms. This is achieved by conditioning the flow on $p > 0$ and on the shrinkage parameter λ . We have then access with one model to (i) the evolution of the posterior for any λ and for any l_p (pseudo-) norms, (ii) the marginal log-likelihood for model selection, and (iii) we can recover the frequentist solution paths as the MAP, which is obtained through simulated annealing.

1 Introduction

Estimating complex relationships between random variables from few observations is a central problem in science. Applications include studying functional connectivity in fMRI data [Smith et al., 2013], networks of interactions from microarray data [Castelo and Roverato, 2006], correlation patterns in longitudinal studies [Diggle, 2002] and many more. Inference about the conditional independence among random variables is particularly relevant. Graphical models are commonly used to represent such independence structure in the form of network graphs. In this work, we focus on Gaussian Graphical Models (GGMs), which are a specific type of undirected graphical models where observations $\mathbf{X} \in \mathbb{R}^{n \times d}$ are assumed to be generated from a multivariate Gaussian distribution $\mathbf{X}_i \sim \mathcal{N}(\boldsymbol{\mu}, \boldsymbol{\Sigma})$ for $i \in \{1, \dots, n\}$, with $\boldsymbol{\mu} \in \mathbb{R}^d$ being the mean and $\boldsymbol{\Sigma} \in \mathbb{R}^{d \times d}$ the covariance matrix. GGMs provide a simple interpretation of conditional independence through the precision matrix $\boldsymbol{\Omega} = \boldsymbol{\Sigma}^{-1}$, whenever $\boldsymbol{\Sigma}$ is non-singular. Specifically, $\Omega_{i,j} = 0$ implies that the pair

of variables (i, j) is conditionally independent given all remaining variables and corresponds to the absence of an edge in the underlying graph.

Penalized likelihood formulation Given the centered observations \mathbf{X} and the associated sample covariance matrix $\mathbf{S} = \mathbf{X}^T \mathbf{X}$, we are interested in reconstructing the precision matrix $\mathbf{\Omega}$, hence the underlying graph structure. This is particularly challenging when $d > n$ because the sample covariance matrix becomes singular and the precision matrix can no longer be obtained by simply inverting the MLE of the covariance matrix. One way to overcome this problem is to consider likelihood-penalized models that encourage sparsity in the precision matrix. We then want to trade off the likelihood with the number of zeros in $\mathbf{\Omega}$, or equivalently the number of edges in the graph:

$$\hat{\mathbf{W}} = \arg \min_{\mathbf{W} \succ 0} \{ \log \det \mathbf{W} - \text{Tr}(\frac{1}{2} \mathbf{S} \mathbf{W}) - \lambda \|\mathbf{W}\|_0 \}, \quad (1)$$

where $\log \det \mathbf{W} - \text{Tr}(\frac{1}{2} \mathbf{S} \mathbf{W})$ is the log-likelihood term and $\|\mathbf{W}\|_0 = \sum_{i < j} 1[w_{ij} \neq 0]$ is the l_0 norm, which simply counts the number of non-zero off-diagonal elements of \mathbf{W} . The trade-off between the two terms is controlled by the parameter $\lambda \geq 0$. Note that the optimization must be performed over the space of symmetric positive definite matrices $\mathbf{W} \succ 0$. In practice, the objective in Eq. (1) is highly non-convex and cannot be easily optimized. Due to the computational hardness of exact l_0 regularization even simpler linear regression settings are restricted to very few features [Hastie et al., 2015]. Similar problems arise for all non-convex sub- l_1 pseudo-norms.

Lasso relaxation: Frequentist and Bayesian approaches In order to simplify Eq. (1), most approaches replace the highly non-convex l_0 norm with the l_1 norm, namely $\|\mathbf{W}\|_1 = \sum_{i < j} |w_{ij}|$, which is the closest convex norm. Meinshausen and Bühlmann [2006] first proposed to employ l_1 regularization in the Graphical Lasso model and sparked the development of several likelihood penalized algorithms [Friedman et al., 2007, Yuan and Lin, 2007, Banerjee et al., 2007]. This frequentist approach allows to elegantly compute the solution path as a function of the shrinkage parameter λ [Mazumder and Hastie, 2012]. The l_1 -relaxed problem can also be easily extended to a Bayesian formulation. Wang [2012] propose to employ a Laplace prior on the off-diagonal elements of the precision matrix and show that the frequentist solution can be recovered as the maximum a posteriori estimate (MAP). Alternative priors have also been proposed [Li et al., 2019]. Bayesian methods allow us to explore the full posterior distribution, to formulate the posterior predictive and to use the marginal likelihood for model selection, but it can be computationally challenging in high-dimensional settings MCMC approximations, for instance, suffer from poor mixing behaviour, which becomes increasingly difficult to diagnose in high dimensions. Furthermore, the Markov chain has to be restarted from scratch for different hyperparameter values. Lastly, Gibbs samplers have become the de-facto standard for Bayesian Lassos, but their dependence on tractable posterior conditionals typically imposes many restrictions on the choice of priors.

Variational Inference Variational methods [Blei et al., 2017] have the potential to overcome many limitations of MCMC samplers. Let \mathbf{x} denote the observed variables and \mathbf{z} the latent unobserved ones. Given a family $\mathcal{Q} = \{q_\theta(\mathbf{z}) | \theta \in \Theta\}$ of parameterized distributions, variational inference consists in finding the distribution $q_{\hat{\theta}}(\mathbf{z})$ that best approximates the posterior $p(\mathbf{z} | \mathbf{x})$. The distance between the two distributions is usually measured in terms of their Kullback-Leibler divergence, which defines the following optimization problem:

$$q_{\hat{\theta}}(\mathbf{z}) = \arg \min_{\theta \in \Theta} \text{KL}(q_\theta(\mathbf{z}) || p(\mathbf{z} | \mathbf{x})) = \arg \min_{\theta \in \Theta} \mathbb{E}_{\mathbf{z} \sim q_\theta} \left[\log \frac{q_\theta(\mathbf{z})}{p(\mathbf{z} | \mathbf{x})} \right]. \quad (2)$$

The goodness of $q_{\hat{\theta}}(\mathbf{z})$ as an approximation of the posterior $p(\mathbf{z} | \mathbf{x})$ creates a trade-off between the expressive power of the variational family \mathcal{Q} and the feasibility of the optimization in Eq. (2). Common approaches rely on the so-called mean field approximation, which assumes mutual independence among variables: $q_\theta(\mathbf{z}) = \prod_i q_{\theta_i}(z_i)$. This is however not possible in GGMs as we intend to model precisely the dependence structure. A few approaches have been proposed for the Bayesian Lasso [Alves et al., 2021] and for its group-sparse variant [Babacan et al., 2014] but, to the best of the authors' knowledge, there exist no work on variational approaches in the context of Bayesian GGMs. Furthermore, there is some evidence that classical variational approaches often result in relatively poor posterior approximations [Turner and Sahani, 2011].

Contribution We present a unified approach to sparse regression for the whole family of all l_p (pseudo-)norms with $0 < p < \infty$, which allows both a fully Bayesian and a frequentist-type interpretation. Specifically, we propose a very general framework for variational inference in Bayesian GGMs through a Normalizing Flow defined over the space of symmetric positive definite matrices. This conditional flow model allows us to simultaneously train a continuum of sparse regression models for all choices of shrinkage parameters $0 < \lambda < \lambda_{\max}$ and all l_p (pseudo-) norms with $0 < p < p_{\max}$. We do so by using as prior the generalized Normal distribution, which recovers the Lasso regularization for $p = 1$ in the MAP limit. As a result, by means of conditioning we have simultaneous access in a single model to posterior inference and to the marginal likelihood as a function of both λ and p . On the one hand, the proposed approach inherits the advantages of the Bayesian framework while avoiding altogether problems arising from Gibbs sampling strategies. On the other hand, it still allows to recover the frequentist solution path as the MAP by training through simulated annealing.

In summary, our main contributions are the following:

1. We propose a general framework for variational inference in GGMs through a normalizing flow defined directly over the space of symmetric positive definite matrices. We condition such a flow on the shrinkage parameter λ and on $p > 0$ to model l_p (pseudo-) norms.
2. This allows to combine the advantages of the Bayesian and frequentist approaches. Within a single model we automatically have access to posterior inference and to the marginal likelihood as a function of both λ and p . We can further recover the frequentist solution path as the MAP by annealing the system.
3. To the best of the authors' knowledge we are the first to propose a unified framework for sub- l_1 pseudo-norms that does not require surrogate penalties and that allows to consistently explore the full solution paths in terms of λ and p .

2 Related Work

In this section we provide an overview of the Bayesian Graphical Lasso and illustrate its limitations. We then motivate the limitations of Lasso regularization and briefly review existing approaches for sparsity with sub- l_1 pseudo-norms. Lastly, as alternative to MCMC approaches, we briefly review normalizing flows for variational inference.

Bayesian Graphical Lasso Along the lines of the Bayesian Lasso by Park and Casella [2008], Wang [2012] provided a Bayesian interpretation of the Graphical Lasso for posterior inference. Specifically, they showed that the l_1 -relaxed optimization of Eq. (1) is equivalent to the maximum a posteriori estimate (MAP) of the model defined by $p(\mathbf{\Omega}|\mathbf{S}, \lambda) \propto p(\mathbf{S}|\mathbf{\Omega}) p(\mathbf{\Omega}|\lambda)$, with

$$\begin{aligned} p(\mathbf{S}|\mathbf{\Omega}) &\propto \mathcal{W}_d(n, \mathbf{\Omega}^{-1}) \\ p(\mathbf{\Omega}|\lambda) &\propto \mathcal{W}_d(d+1, \lambda \mathbf{1}_d) \prod_{i < j} \text{DE}(\omega_{ij}|\lambda) I[\mathbf{\Omega} \succ 0], \end{aligned} \quad (3)$$

where the indicator function $I[\mathbf{\Omega} \succ 0]$ imposes positive definiteness on the precision matrix $\mathbf{\Omega}$. Since $\mathbf{X}_i \sim \mathcal{N}(\boldsymbol{\mu}, \mathbf{\Omega}^{-1})$, the sample covariance matrix $\mathbf{S} = \mathbf{X}^T \mathbf{X}$ is distributed according to the Wishart distribution $\mathcal{W}_d(n, \mathbf{\Omega}^{-1}) \propto \det(\mathbf{\Omega})^{n/2} \det(\mathbf{S})^{(n-d-1)/2} \exp \text{Tr}(-\frac{1}{2} \mathbf{\Omega} \mathbf{S})$, which explains the likelihood term. The Wishart distribution is further used in the prior to impose symmetry and positive definiteness on $\mathbf{\Omega}$, which actually simplifies to $\mathcal{W}_d(d+1, \lambda \mathbf{1}_d) \propto \prod_{i=1}^d \frac{\lambda}{2} \exp\{-\frac{\lambda}{2} \omega_{ii}\}$. Furthermore, Wang [2012] proposed to employ a Laplace prior $\text{DE}(\omega_{ij}|\lambda) = \frac{\lambda}{2} \exp\{-\lambda |\omega_{ij}|\}$ on the off-diagonal elements of $\mathbf{\Omega}$ to encourage sparsity.

The main limitations of this approach can be traced back to restrictions imposed by the use of a Gibbs sampler, which is computationally expensive and can suffer from high rejection rates, especially in high-dimensions [Mohammadi and Wit, 2015]. Furthermore, to recover the frequentist solution path as a function of λ the Markov Chain must be restarted for each λ values. Lastly, the derivation of the Gibbs sampler itself is specific to the prior in Eq. (3) and cannot be easily generalized to other priors. Its derivation also requires to expand the Laplace prior as an infinite mixture of Gaussians [Andrews and Mallows, 1974, West, 1987] and to define an ad-hoc mixing density.

Sparsity with sub- l_1 pseudo-norms In the penalized likelihood framework, sparsity is formalized through the l_0 norm because it directly penalizes the non-zero entries and is thus equivalent to best subset selection of the variables. The convex relaxation with the l_1 norm makes the problem tractable but comes at the cost of encouraging shrinkage of the retained variables as well [Hastie et al., 2015]. This motivates interest in sub- l_1 pseudo-norms, which in the limit reduce to the original l_0 norm formulation. However, due to their non-convexity and combinatorial complexity multiple alternative penalties have been proposed. Notably, we do not have to resort to alternative penalties as we can directly and exactly enforce sub- l_1 pseudo-norms regularization through a suitable prior. We provide a quick overview of the main algorithms in the context of linear regression. The popular SCAD [Fan and Li, 2001] guarantees unbiasedness, sparsity, and continuity while reducing the over-shrinking behaviour. Zhang [2010] proposed the nearly unbiased MC+ method, which consists of a concave penalty plus a selection algorithm that allows to bridge the gap between l_1 and l_0 . Mazumder et al. [2011] provide a coordinate-descent algorithm to find the solution path within the sub- l_1 space for several non-convex penalties. Recently, more efficient algorithms that solve higher dimensional problems have been proposed [Bertsimas et al., 2015]. In the Bayesian framework, Ishwaran and Rao [2005] proposed to use a rescaled spike and slab prior to encourage variable selection and drew connections to Ridge regularization.

Normalizing Flows for variational inference Normalizing Flows (NFs) are powerful and flexible models that allow to perform accurate density estimation and, at the same time, to sample from such a density for free. For this reason, NFs provide a very attractive solution to perform efficient and powerful variational inference [Rezende and Mohamed, 2015, van den Berg et al., 2019]. Suppose $\mathbf{X} \in \mathbb{R}^d$ is a continuous random variable with unknown distribution $p_{\mathbf{X}} : \mathbb{R}^d \mapsto \mathbb{R}$ and let $\mathbf{Z} \in \mathbb{R}^d$ be any continuous random variable with any known $\mathbf{Z} \sim p_{\mathbf{Z}} : \mathbb{R}^d \mapsto \mathbb{R}$, which we refer to as the base distribution. The idea at the core of NFs is to construct a diffeomorphism $\mathcal{T} : \mathbf{X} \mapsto \mathbf{Z}$, i.e. a differentiable bijection, in order to re-write $p_{\mathbf{X}}$ through the change of variable formula as

$$p_{\mathbf{X}}(\mathbf{x}) = p_{\mathbf{Z}}(\mathcal{T}(\mathbf{x})) |\det \mathcal{J}_{\mathcal{T}}(\mathbf{x})|, \quad (4)$$

where $\mathcal{J}_{\mathcal{T}}$ is the Jacobian of the transformation \mathcal{T} . Assuming we have successfully learnt the transformation \mathcal{T} , we can then evaluate exactly the target density through Eq. (4) and generate samples from it by simply transforming samples from the base distribution through \mathcal{T} , namely $\mathbf{X} = \mathcal{T}(\mathbf{Z})$ with $\mathbf{Z} \sim p_{\mathbf{Z}}$. In practice, the crucial part in designing NFs is how to construct arbitrarily complicated bijections. The key idea is to exploit the property that compositions $\mathcal{T} = \mathcal{T}_1 \circ \dots \circ \mathcal{T}_m$ of bijections $\{\mathcal{T}_i\}_{i=1}^m$ remain bijections. Relevantly, the determinant of the Jacobian of the resulting transformation can be expressed trivially in terms of the determinant of each \mathcal{T}_i as

$$\det \mathcal{J}_{\mathcal{T}}(\mathbf{x}) = \prod_{i=1}^m \det \mathcal{J}_{\mathcal{T}_i}(\mathbf{u}_{i-1}) \quad \text{with} \quad \mathbf{u}_{i-1} = \mathcal{T}_1(\mathbf{x}) \circ \dots \circ \mathcal{T}_{i-1}(\mathbf{u}_{i-2}). \quad (5)$$

Therefore, through the composition of computationally tractable non-linear bijections, it is possible to define arbitrarily expressive bijections and hence to transform the base distribution $p_{\mathbf{Z}}$ into arbitrarily complicated distributions $p_{\mathbf{X}}$. Among others, Huang et al. [2018] proved that autoregressive flows are universal density approximators of continuous random variables. For a comprehensive review of NFs and their different architectures see Papamakarios et al. [2021] and Kobyzev et al. [2020]. As first proposed by Atanov et al. [2020], it is also possible to condition the transformation \mathcal{T} on some parameter $c \in \mathbb{R}^n$. The resulting Conditional Normalizing Flow [Kobyzev et al., 2020] allows then to model with one flow the family of conditional distributions $p_{\mathbf{X}}(\mathbf{x}|c)$ for continuous values of c .

3 Proposed approach

We now describe how to infer the posterior of Ω in GGMs with conditional NFs and how to do so as a function of the shrinkage parameter λ and of p for l_p (pseudo-) norm regularization, all within a single model. We argue that NFs are particularly suited because they allow to efficiently infer the posterior and they directly provide the marginal likelihood for model selection. On top of these advantages of the Bayesian perspective, we further show how to recover the frequentist solution path by simply training through simulated annealing.

3.1 Generalized Normal distribution for l_p (pseudo-)norms

Unlike previous Bayesian approaches to GGMs, we can flexibly specify any prior (and likelihood) in Eq. (3) and this allows us to extend the model beyond the standard l_1 relaxation. Wang [2012] showed that a Laplace prior on the off-diagonal elements of Ω is equivalent in the MAP limit to l_1 likelihood regularization. We generalize this idea to any l_p (pseudo-) norm by employing the generalized Normal distribution as prior, which reduces to the Laplace and Normal distribution as two special case. Its probability density function is defined as:

$$f(x|q, p) = \frac{p}{2q\Gamma(1/p)} \exp\left\{-\frac{|x|^p}{q^p}\right\}, \quad (6)$$

where $\Gamma(\cdot)$ is the Gamma function, $q, p > 0$ are the scale and shape parameter, respectively. We assume the distribution to be centered around zero, i.e. $\mu = 0$. If we now consider the log-probability and drop the normalization constant, which does not affect the KL optimization, we recover the l_p (pseudo-) norm. To see this it is sufficient to define $\lambda = q^{-1} > 0$. Our full model is thus conditioned through the prior on both λ and on p and is defined as $p(\Omega|\mathbf{S}, \lambda, p) \propto p(\mathbf{S}|\Omega) p(\Omega|\lambda, p)$ with

$$\begin{aligned} p(\mathbf{S}|\Omega) &\propto \mathcal{W}_d(n, \Omega^{-1}) \\ p(\Omega|\lambda, p) &\propto \mathcal{W}_d(d+1, \lambda \mathbf{1}_d) \prod_{i < j} \frac{p\lambda}{2\Gamma(1/p)} \exp\{-\lambda^p |\omega_{ij}|^p\} I[\Omega \succ 0]. \end{aligned} \quad (7)$$

Note that for $p = 1$ the prior on the off-diagonals reduces to the Laplace distribution and the exact formulation of Eq. (3) is recovered, i.e. Lasso regularization. For $p = 2$ we recover instead the Normal distribution, i.e. Ridge regularization. Overall, when employing the distribution in Eq. (7), we can effectively model solutions corresponding to l_p (pseudo-) norm regularization for $p > 0$, including the non-convex sub- l_1 pseudo-norms.

3.2 Variational inference with conditional flows for GGMs

As we want to model the posterior $p(\Omega|\mathbf{S})$ over the precision matrix Ω , we design flows directly over the space of symmetric positive definite matrices. Specifically, as we want to study the evolution of the posterior as a function of the shrinkage parameter λ and of the p for l_p (pseudo-) norms regularization, we train a NF conditioned on $\lambda \in [\lambda_1, \lambda_2]$ and on $p \in [p_1, p_2]$ for any user-defined $\lambda_1, \lambda_2, p_1, p_2 > 0$. From Eq. (4) the resulting flow $\mathcal{T}_{\theta(\lambda, p)}$ implicitly defines the probability $p_{\theta(\lambda, p)}(\Omega) = p_{base}(\mathcal{T}_{\theta(\lambda, p)}(\Omega)) |\det \mathcal{J}_{\mathcal{T}_{\theta(\lambda, p)}(\Omega)}|$, which we want to train to approximate the (unnormalized) posterior $p^*(\mathbf{X}|\Omega, \lambda, p) = p(\Omega|\mathbf{X}) p(\Omega|\lambda, p)$. Similarly to Eq. (2), we define our objective function to be the reverse KL divergence the variational probability $p_{\theta(\lambda, p)}(\Omega)$ implicitly defined by the flow $\mathcal{T}_{\theta(\lambda, p)}$:

$$\begin{aligned} \mathcal{L}(\theta; \lambda, p) &= \text{KL}(p_{\theta(\lambda, p)}(\Omega) || p^*(\mathbf{X}|\Omega, \lambda, p)) \\ &\approx \frac{1}{M} \sum_{i=1}^M \log \frac{p_{\theta(\lambda, p)}(\Omega_i)}{p^*(\mathbf{X}|\Omega_i, \lambda, p)}. \end{aligned} \quad (8)$$

In practice, the expectation is approximated with Monte Carlo sampling. Note that this is particularly efficient in NFs because it only requires to sample from the base distribution $p_{base}(\mathcal{T}_{\theta(\lambda, p)}(\Omega))$, which is trivial. We further need to evaluate the unnormalized posterior $p^*(\mathbf{X}|\Omega, \lambda, p)$, but this is also trivial since we know the analytic form of the likelihood and of the prior. Relevantly, in Eq. (8) we do not require the normalizing constant $N_C(\lambda, p) = p^*(\mathbf{X}|\Omega, \lambda, p)/p(\mathbf{X}|\Omega, \lambda, p)$ because it does not influence the optimization.

3.3 Conditional Matrix Flow

We now describe how we design the proposed conditional normalizing flow and how we define it over the space of symmetric precision matrices by construction. We exploit the well-known Cholesky decomposition [Horn and Johnson, 1985], which states that for any symmetric positive definite matrix $\mathbf{M} \in \mathbb{R}^{d \times d}$ there exists a unique decomposition $\mathbf{M} = \mathbf{L}\mathbf{L}^T$, and viceversa. $\mathbf{L} \in \mathbb{R}^{d \times d}$ is a lower triangular matrix with positive diagonal elements, which is fully defined by $d(d+1)/2$ non-zero elements. In other words, we need $d(d+1)/2$ degrees of freedom, hence a $d(d+1)/2$ -dimensional

flow, to describe a symmetric positive definite matrix. We now illustrate how to transform the initial $\mathbf{z} \in \mathbb{R}^{d(d+1)/2}$ vector into a symmetric positive definite matrix $\mathbf{\Omega} \in \mathbb{R}^{d \times d}$. To the best of the authors' knowledge, this is the first attempt to define a flow $\mathcal{T}(\mathbf{\Omega})$ on the space of symmetric positive definite matrices by construction. A high-level visualization of the proposed architecture is given in Figure 1.

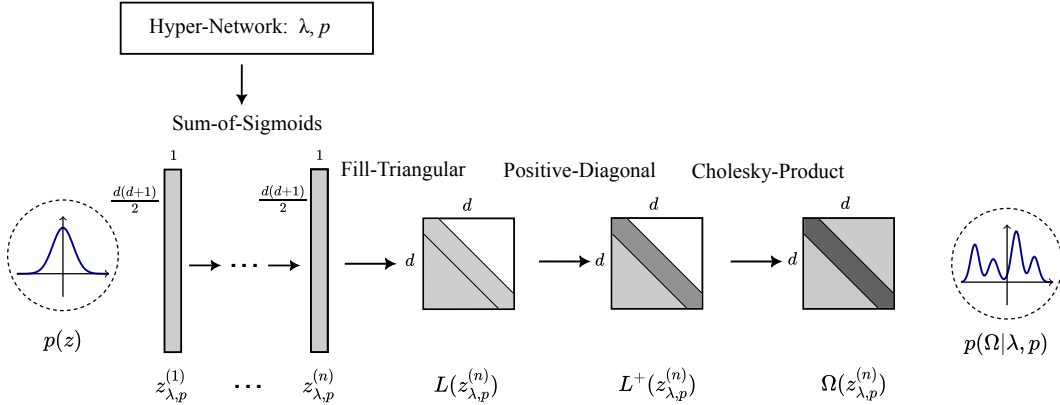


Figure 1: Architecture of the proposed Conditional Matrix Flow model. Light grey is used to denote unconstrained values, darker greys for positive values and white for zeros.

The first n layers of the network consist of the proposed Sum-of-Sigmoids transformations and map the initial vector \mathbf{z} to $\mathbf{z}_{\lambda, p}^{(n)}$. We provide further insight on how these layers are implemented in Appendix A. As these transformations are unconstrained the Sum-of-Sigmoids can be replaced by any Normalizing Flow architecture of choice. Furthermore, we condition the flow on λ and p via a Hyper-Network. The Hyper-Network takes λ and p as inputs and returns the parameters of the Matrix Flow. In practice, we implement this high-level structure based on the code provided by the *nflows* library [Durkan et al., 2020]. To transform $\mathbf{z}_{\lambda, p}^{(n)}$ into a symmetric positive definite matrix we use three bijective layers. First, the vector is raveled into a lower triangular matrix $\mathbf{L} \in \mathbb{R}^{d \times d}$, which we denote by *Fill-Triangular*. This transformation has a unit Jacobian determinant because it just reshapes the vector into a matrix. In a second step we bijectively map the diagonal of the resulting lower triangular matrix to positive values with a softplus activation $\text{Softplus}(\mathbf{x}) = \log(1 + \exp \mathbf{x})$. This transformation, which we refer to as *Positive-Diagonal*, acts element-wise and hence admits a cheap Jacobian (log)-determinant. Lastly, we compute the *Cholesky product* $\text{Chol}(\mathbf{L}) : \mathbf{L} \mapsto \mathbf{L}\mathbf{L}^T$, which again has an inexpensive Jacobian (log-) determinant [Gupta and Nagar, 1999]:

$$\det \mathcal{J}_{\text{Chol}}(\mathbf{L}) = 2^d \prod_{i=1}^d (\mathbf{L}_{ii})^{d-i+1}, \quad (9)$$

which depends only on the d diagonal elements of \mathbf{L} .

3.4 Model selection through marginal likelihood

Differently from standard Bayesian approaches, the proposed conditional flow provides access directly to the marginal log-likelihood $\log p(\mathbf{X}|\lambda)$ as a function of λ without any further calculations. This is particularly interesting because the marginal log-likelihood is extremely expensive to compute with classical approaches. To see how we have automatically access to the marginal log-likelihood, consider the objective function in Eq. (8) for a fixed $\hat{\lambda}$:

$$\mathcal{L}(\theta(\hat{\lambda})) = \text{KL}(p_{\theta(\hat{\lambda})}(\mathbf{\Omega}) || p^*(\mathbf{X}|\mathbf{\Omega}, \hat{\lambda})) = \text{KL}(p_{\theta(\hat{\lambda})}(\mathbf{\Omega}) || p(\mathbf{\Omega}|\mathbf{X}, \hat{\lambda})) - \log p(\mathbf{X}|\hat{\lambda}) \quad (10)$$

For clarity, we have momentarily dropped the dependence on p . The second equality follows from Bayes formula $p(\mathbf{\Omega}|\mathbf{X}, \hat{\lambda}) = \frac{p^*(\mathbf{X}|\mathbf{\Omega}, \hat{\lambda})}{p(\mathbf{X}|\hat{\lambda})}$ with $p(\mathbf{X}|\hat{\lambda}) = \int p^*(\mathbf{X}|\mathbf{\Omega}, \hat{\lambda}) d\mathbf{\Omega} = \int p(\mathbf{X}|\mathbf{\Omega}) p(\mathbf{\Omega}|\hat{\lambda}) d\mathbf{\Omega}$. If we assume that the flow is expressive enough and that the optimization reached the global minimum, we can consider the Kullback-Leibler divergence to be practically zero. In this case the loss function at the end of training gives us access directly to the marginal log-likelihood for any continuous value of λ . We can then perform model selection by simply choosing $\lambda^* = \min_{\lambda} \mathcal{L}(\theta(\lambda)) = \max_{\lambda} \log p(\mathbf{X}|\lambda)$.

3.5 Training through simulated annealing

With the proposed conditional flow model, we are able to perform posterior inference as a function of λ and p and to perform model selection, which are key advantages of the Bayesian perspective. We now show how to also recover the frequentist solution path as a function of λ without modifying the model. We employ optimization through Simulated Annealing [Kirkpatrick et al., 1983] to approximately sample from the global maxima of the distribution, which for posteriors is the maximum a posteriori estimate (MAP). The idea comes from statistical mechanics, where slowly cooling processes are used to study the ground (optimal) state of the system. When applied to more general optimization tasks, simulated annealing consists in accepting iterative improvements if they lead to a lower cost function. Meanwhile, the temperature is slowly decreased from the initial value T_0 to practically $T_n = 0$, where the system is frozen and no further changes occur. In our setting this corresponds to introducing an artificial temperature T_i for the posterior in Eq. (7):

$$p_i^*(\Omega) = p^*(\mathbf{X}|\Omega, \lambda)^{1/T_i} \quad (11)$$

where T_i is the temperature at the i -th iteration. If the initial temperature is high enough, $p_i^*(\Omega)$ will likely be very flat while as the temperature decreases the distribution becomes more peaked. In the limit $T_n \rightarrow 0$ the distribution $p_i^*(\Omega)$ should concentrate on the global maximum, hence on the MAP solution. Geman and Geman [1984] formally showed that convergence to the set of global minima is guaranteed for logarithmic cooling schedules. Unfortunately, logarithmic cooling schedule are not viable in practice, so alternative schemes have been explored in the literature [Abramson et al., 1999]. In this work we use the popular geometric cooling schedule [Andrieu and Doucet, 2000, Yuan et al., 2012], which works well in practice: $T_i = T_0 a^i$ for some $a > 0$ and $i \in \{1, \dots, n\}$. In practice, we train the objective in Eq. (8) while slowly cooling down the system, i.e. decreasing T_i in Eq. (11), until we reach a sufficiently low temperature T_n . By saving the model at $T_i = 1$ and T_n we have access to the results provided by both the Bayesian and frequentist approaches, respectively.

4 Experiments

In this section we showcase the effectiveness of the proposed approach first on artificial data and then on a real application. In particular, we study the evolution of the variational posterior as a function of λ and p . This also gives us access to the marginal likelihood, which we use to perform model selection on λ . We further illustrate the effect of training through simulated annealing and how it allows to recover the frequentist solution path through the MAP. Lastly, we show that the proposed method can be readily applied to real data in higher dimensional settings.

4.1 Artificial data

We illustrate the proposed model on an artificial dataset of sparse precision matrices. The data generation process consists in sampling a precision matrix, compute the covariance matrix by inversion and then generate Gaussian data accordingly. We employ a sparse precision matrix generator [Pedregosa et al., 2011] that allows to choose the number of features d and of the amount of sparsity α . In this toy example, we choose $n > d$ to ensure the invertibility of the empirical covariance. We trained our model on a wide range of d , n , and α values and observed consistent behaviour. For illustrative purposes we report results for $n = 500$, $d = 15$, and $\alpha = 80\%$.

We trained our model for 4000 epochs through simulated annealing with an initial temperature of $T_0 = 5$ to $T_n = 0.01$ and performed 80 steps of geometric cooling schedule $T_i = T_0 a^i$ for $a = T_n/T_0$. In Figure 2 we show the effect of simulated annealing on the posterior. At temperature $T = 1$ the conditional flow approximates the true posterior in Eq. (7), which for $p = 1$ coincides to the Bayesian Graphical Lasso. As we decrease the temperature, the unnormalized posterior in Eq. (11) becomes more peaked and we observe credible intervals getting progressively more shrunk. As we reach the final temperature T_n , the distribution is peaked on the MAP and we recover the frequentist path. The model provides accurate reconstruction of the solution path over λ (MSE = 0.0046). Furthermore, we perform model selection on λ for the model in Eq. (7), which is obtained at temperature $T = 1$. In Figure 3 (left) we show the marginal log-likelihood as a function of λ and the resulting optimal $\lambda^* = 0.044$ that maximizes it. We compare the result with the frequentist estimate obtained through 5-fold cross validation $\lambda_{cv}^* = 0.026$. Also in this case the model agrees with the frequentist solution. Lastly, we explore the behaviour of the posterior as a function of p ,

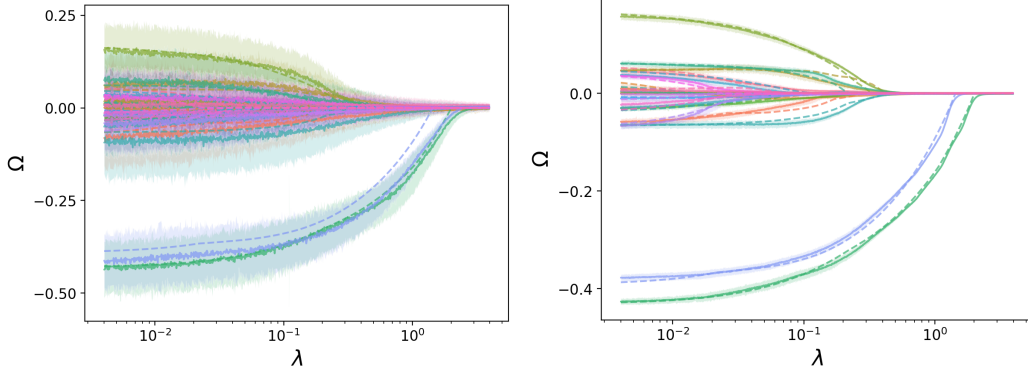


Figure 2: 95% posterior credible intervals solution path as a function of λ for $p = 1$. At $T = 1$ we recover the Bayesian Graphical Lasso (left) and at $T = 0.01$ we recover the Graphical Lasso (right). The dashed line is the Graphical Lasso solution path.

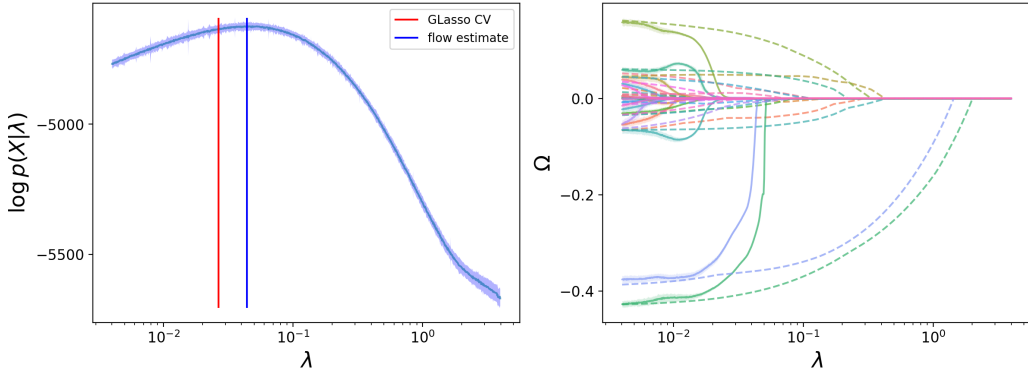


Figure 3: Left: Evolution of the marginal log-likelihood as a function of λ for $T = 1$ and $p = 1$. We compare the optimal λ (blue) with frequentist estimate obtained through CV (red). Right: MAP estimate as a function of λ for $p = 0.5$. The dashed line is the frequentist solution path for $p = 1$.

specifically in the sub- l_1 pseudo-norm regime. In order to have the Lasso solution path as reference, we compare different p values in the annealed system at $T = 0.01$. In Figure 3 (right) we show 95% credible intervals for the posterior for $p = 0.5$. Compared to the l_1 solution path, we observe that sub- l_1 solution paths stay constant for longer and then rapidly shrink towards zero. This behaviour becomes more evident as p decreases, as we show in the Appendix A. This overcomes one of the main limitations of Lasso regularization, namely that in order to achieve sparsity the selected features are over-shrunk. These results support the interest in sub- l_1 pseudo-norms, and l_0 norm in the limit.

4.2 Real data application

We showcase the practical significance of the proposed approach on a more challenging real world setting. We consider the problem of identifying connections between gene expression measurements and clinical descriptors. In particular, we use the colorectal cancer dataset [Sheffer et al., 2009], which contain measurements of 7 clinical variables together with 312 gene measurements from biopsies for 260 cancer patients. As the dataset contains many missing values, we drop the *p53 mutation status* clinical variable and we consider $n = 190$ fully measured patients. Our goal is to study the connections between the $s = 6$ clinical variables and the $t = 312$ gene expression measurements. Similarly to Kaufmann et al. [2015], we consider the partition

$$\Omega = \begin{pmatrix} \Omega_{11} & \Omega_{12} \\ \Omega_{12}^T & \Omega_{22} \end{pmatrix} \begin{matrix} s \\ t \end{matrix} \quad \mathbf{S} = \begin{pmatrix} \mathbf{S}_{11} & \mathbf{S}_{12} \\ \mathbf{S}_{12}^T & \mathbf{S}_{22} \end{pmatrix} \begin{matrix} s \\ t \end{matrix} \quad (12)$$

and instead of inferring the full $(s+t) \times (s+t)$ precision matrix Ω , we study the $s \times (s+t)$ sub-matrix Ω_{12} . Inspired by Kaufmann et al. [2015], we show in Appendix A that we can infer the posterior $p(\Omega_{11}, \Omega_{12} | \mathcal{S}, \lambda)$ independently of the large $\Omega_{22,1}$. In contrast to Kaufmann et al. [2015], we can enforce the correct double-exponential prior on Ω_{11} , we do not need to invert the $st \times st$ matrix which takes $O(st^3)$ operations, and can still suffer from poor mixing behaviour. Within the proposed framework we only need to define a different unnormalized posterior as the target distribution. In practice, we define the flow jointly over the sub-matrices Ω_{11} , which must be positive definite, and Ω_{12} , which is unconstrained. It is then sufficient to define the bijective layers over $s(s+1)/2$ plus $s \times t$ dimensions and to perform the Cholesky product only on the dimensions encoding Ω_{11} . Note that the determinant of the Jacobian of the full transformation is still the same as in Eq. (9) because the $s \times t$ dimensions encoding Ω_{12} are just raveled into a matrix.

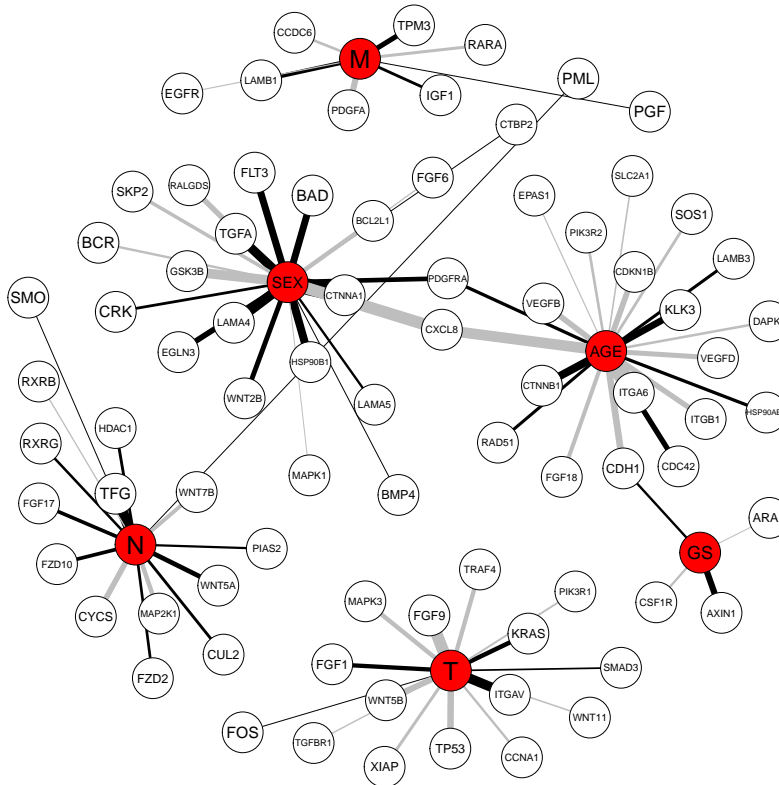


Figure 4: Inferred network structure between clinical variables and gene expression measurements.

In Figure 4 we show the resulting network structure between the clinical variables and gene expression measurements. This is obtained by considering 99% credible intervals on the posterior of Ω_{12} . We further provide an interpretation of the result in terms of known confounding effects. The clinical variables in the data are age, sex, cancer group stage (GS) and the TNM classification for colorectal cancer, which measures its size (T), whether it spread to lymph nodes (N) and if it developed metastases (M). Among these, age, sex and tumor size show the strongest connections with gene measurements. However, age and sex are not particularly interesting from a clinical standpoint. We thus focus our attention on the tumor size variable (T). We observe strong links to Fibroblast growth factors (FGF1, FGF9) which are known to have an important role in tumor angiogenesis and to promote cancer progression [Compagni et al., 2000, Chang et al., 2018]. Further, we find a strong link to the heterodimeric integral membrane ITGAV, which has been reported to be a strong predictor for prognosis in colorectal cancer [J et al., 2014].

5 Conclusions

We propose a very general framework for variational inference in Gaussian Graphical Models through conditional normalizing flows. The proposed model unifies the benefits of both Bayesian and frequentist approaches, while avoiding most of their specific problems. Compared with existing approaches, the most important advantage of our method is the possibility to jointly train a continuum of sparse regression models jointly for all regularization parameters and all l_p (pseudo-) norms. All of these models can be analyzed both in a Bayesian fashion (at temperature $T = 1$) or, alternatively, in the frequentist (i.e. penalized likelihood) limit as T approaches 0. To our best knowledge, we present the first Gaussian network model that allows for a continuous exploration of all sparsity-inducing priors from the l_p -norm family. Moreover, due to our variational formalism, we can integrate out the model parameters and use the (approximate) marginal likelihood for model selection without any additional computational costs.

References

- Stephen M. Smith, Christian F. Beckmann, Jesper Andersson, Edward J. Auerbach, Janine Bijsterbosch, Gwenaëlle Douaud, Eugene Duff, David A. Feinberg, Ludovica Griffanti, Michael P. Harms, Michael Kelly, Timothy Laumann, Karla L. Miller, Steen Moeller, Steve Petersen, Jonathan Power, Gholamreza Salimi-Khorshidi, Abraham Z. Snyder, An T. Vu, Mark W. Woolrich, Junqian Xu, Essa Yacoub, Kamil Uğurbil, David C. Van Essen, and Matthew F. Glasser. Resting-state fmri in the human connectome project. *NeuroImage*, 80:144–168, 2013. ISSN 1053-8119. doi: <https://doi.org/10.1016/j.neuroimage.2013.05.039>. URL <https://www.sciencedirect.com/science/article/pii/S1053811913005338>. Mapping the Connectome.
- Robert Castelo and Alberto Roverato. A robust procedure for gaussian graphical model search from microarray data with p larger than n. *Journal of Machine Learning Research*, 7(94):2621–2650, 2006. URL <http://jmlr.org/papers/v7/castelo06a.html>.
- P. Diggle. *Analysis of Longitudinal Data*. Oxford Statistical Science Series. OUP Oxford, 2002. ISBN 9780198524847. URL <https://books.google.it/books?id=kKLbyWycRwc>.
- Trevor Hastie, Robert Tibshirani, and Martin Wainwright. *Statistical Learning with Sparsity: The Lasso and Generalizations*. Chapman & Hall/CRC, 2015. ISBN 1498712169.
- Nicolai Meinshausen and Peter Bühlmann. High-dimensional graphs and variable selection with the Lasso. *The Annals of Statistics*, 34(3):1436 – 1462, 2006. doi: 10.1214/009053606000000281. URL <https://doi.org/10.1214/009053606000000281>.
- Jerome Friedman, Trevor Hastie, and Robert Tibshirani. Sparse inverse covariance estimation with the graphical lasso. *Biostatistics*, 9(3):432–441, 12 2007. ISSN 1465-4644. doi: 10.1093/biostatistics/kxm045. URL <https://doi.org/10.1093/biostatistics/kxm045>.
- Ming Yuan and Yi Lin. Model selection and estimation in the gaussian graphical model. *Biometrika*, 94(1):19–35, 2007. ISSN 00063444, 14643510. URL <http://www.jstor.org/stable/20441351>.
- Onureena Banerjee, Laurent El Ghaoui, and Alexandre d’Aspremont. Model selection through sparse maximum likelihood estimation, 2007.
- Rahul Mazumder and Trevor Hastie. The graphical lasso: New insights and alternatives. *Electronic Journal of Statistics*, 6(none):2125 – 2149, 2012. doi: 10.1214/12-EJS740. URL <https://doi.org/10.1214/12-EJS740>.
- Hao Wang. Bayesian Graphical Lasso Models and Efficient Posterior Computation. *Bayesian Analysis*, 7(4):867 – 886, 2012. doi: 10.1214/12-BA729. URL <https://doi.org/10.1214/12-BA729>.
- Yunfan Li, Bruce A. Craig, and Anindya Bhadra. The graphical horseshoe estimator for inverse covariance matrices, 2019.
- David M. Blei, Alp Kucukelbir, and Jon D. McAuliffe. Variational inference: A review for statisticians. *Journal of the American Statistical Association*, 112(518):859–877, apr 2017. doi: 10.1080/01621459.2017.1285773. URL <https://doi.org/10.1080%2F01621459.2017.1285773>.
- Larissa Alves, Ronaldo Dias, and Helio S. Migon. Variational full bayes lasso: Knots selection in regression splines, 2021.
- S. Derin Babacan, Shinichi Nakajima, and Minh N. Do. Bayesian group-sparse modeling and variational inference. *IEEE Transactions on Signal Processing*, 62(11):2906–2921, 2014. doi: 10.1109/TSP.2014.2319775.
- R. E. Turner and M. Sahani. Two problems with variational expectation maximisation for time-series models. In D. Barber, T. Cemgil, and S. Chiappa, editors, *Bayesian Time series models*, chapter 5, pages 109–130. Cambridge University Press, 2011.
- Trevor Park and George Casella. The bayesian lasso. *Journal of the American Statistical Association*, 103(482):681–686, 2008. doi: 10.1198/016214508000000337. URL <https://doi.org/10.1198/016214508000000337>.

- A. Mohammadi and E. C. Wit. Bayesian Structure Learning in Sparse Gaussian Graphical Models. *Bayesian Analysis*, 10(1):109 – 138, 2015. doi: 10.1214/14-BA889. URL <https://doi.org/10.1214/14-BA889>.
- D. F. Andrews and C. L. Mallows. Scale mixtures of normal distributions. *Journal of the Royal Statistical Society. Series B (Methodological)*, 36(1):99–102, 1974. ISSN 00359246. URL <http://www.jstor.org/stable/2984774>.
- Mike West. On scale mixtures of normal distributions. *Biometrika*, 74(3):646–648, 09 1987. ISSN 0006-3444. doi: 10.1093/biomet/74.3.646. URL <https://doi.org/10.1093/biomet/74.3.646>.
- Jianqing Fan and Runze Li. Variable selection via nonconcave penalized likelihood and its oracle properties. *Journal of the American Statistical Association*, 96:1348–1360, 02 2001. doi: 10.1198/016214501753382273.
- Cun-Hui Zhang. Nearly unbiased variable selection under minimax concave penalty. *The Annals of Statistics*, 38(2):894 – 942, 2010. doi: 10.1214/09-AOS729. URL <https://doi.org/10.1214/09-AOS729>.
- Rahul Mazumder, Jerome H. Friedman, and Trevor Hastie. Sparsenet: Coordinate descent with non-convex penalties. *Journal of the American Statistical Association*, 106(495):1125–1138, 2011. doi: 10.1198/jasa.2011.tm09738. URL <https://doi.org/10.1198/jasa.2011.tm09738>. PMID: 25580042.
- Dimitris Bertsimas, Angela King, and Rahul Mazumder. Best subset selection via a modern optimization lens, 2015.
- Hemant Ishwaran and J. Sunil Rao. Spike and slab variable selection: Frequentist and bayesian strategies. *The Annals of Statistics*, 33(2), apr 2005. doi: 10.1214/009053604000001147. URL <https://doi.org/10.1214/009053604000001147>.
- Danilo Rezende and Shakir Mohamed. Variational inference with normalizing flows. In Francis Bach and David Blei, editors, *Proceedings of the 32nd International Conference on Machine Learning*, volume 37 of *Proceedings of Machine Learning Research*, pages 1530–1538, Lille, France, 07–09 Jul 2015. PMLR. URL <https://proceedings.mlr.press/v37/rezende15.html>.
- Rianne van den Berg, Leonard Hasenclever, Jakub M. Tomczak, and Max Welling. Sylvester normalizing flows for variational inference, 2019.
- Chin-Wei Huang, David Krueger, Alexandre Lacoste, and Aaron Courville. Neural autoregressive flows, 2018.
- George Papamakarios, Eric Nalisnick, Danilo Jimenez Rezende, Shakir Mohamed, and Balaji Lakshminarayanan. Normalizing flows for probabilistic modeling and inference. *J. Mach. Learn. Res.*, 22(1), jan 2021. ISSN 1532-4435.
- Ivan Kobyzev, Simon Prince, and Marcus Brubaker. Normalizing flows: An introduction and review of current methods. *IEEE Transactions on Pattern Analysis and Machine Intelligence*, PP:1–1, 05 2020. doi: 10.1109/TPAMI.2020.2992934.
- Andrei Atanov, Alexandra Volokhova, Arsenii Ashukha, Ivan Sosnovik, and Dmitry Vetrov. Semi-conditional normalizing flows for semi-supervised learning, 2020.
- Roger A. Horn and Charles R. Johnson. *Matrix analysis / Roger A. Horn, Charles R. Johnson*. Cambridge University Press Cambridge [Cambridgeshire] ; New York, repr. with corr. edition, 1985. ISBN 0521305861 0521386322. URL <http://www.loc.gov/catdir/toc/cam023/85007736.html>.
- Conor Durkan, Artur Bekasov, Iain Murray, and George Papamakarios. nflows: normalizing flows in PyTorch, November 2020. URL <https://doi.org/10.5281/zenodo.4296287>.
- Arjun K Gupta and Daya K Nagar. *Matrix variate distributions*, volume 104. CRC Press, 1999.

- S. Kirkpatrick, C. D. Gelatt, and M. P. Vecchi. Optimization by simulated annealing. *Science*, 220 (4598):671–680, 1983. doi: 10.1126/science.220.4598.671. URL <https://www.science.org/doi/abs/10.1126/science.220.4598.671>.
- Stuart Geman and Donald Geman. Stochastic relaxation, gibbs distributions, and the bayesian restoration of images. *IEEE Transactions on Pattern Analysis and Machine Intelligence*, PAMI-6 (6):721–741, 1984. doi: 10.1109/TPAMI.1984.4767596.
- David Abramson, Mohan Krishnamoorthy, and Henry Dang. Simulated annealing cooling schedules for the school timetabling problem. *Asia-Pacific Journal of Operational Research*, pages 1 – 22, 1999. ISSN 0217-5959.
- Christophe Andrieu and Arnaud Doucet. Simulated annealing for maximum a posteriori parameter estimation of hidden markov models. *Information Theory, IEEE Transactions on*, 46:994 – 1004, 06 2000. doi: 10.1109/18.841176.
- Changhe Yuan, Tsai-Ching Lu, and Marek J. Druzdzal. Annealed map, 2012.
- F. Pedregosa, G. Varoquaux, A. Gramfort, V. Michel, B. Thirion, O. Grisel, M. Blondel, P. Prettenhofer, R. Weiss, V. Dubourg, J. Vanderplas, A. Passos, D. Cournapeau, M. Brucher, M. Perrot, and E. Duchesnay. Scikit-learn: Machine learning in Python. *Journal of Machine Learning Research*, 12:2825–2830, 2011.
- Michal Sheffer, Manny D. Bacolod, Or Zuk, Sarah F. Giardina, Hanna Pincas, Francis Barany, Philip B. Paty, William L. Gerald, Daniel A. Notterman, and Eytan Domany. Association of survival and disease progression with chromosomal instability: A genomic exploration of colorectal cancer. *Proceedings of the National Academy of Sciences*, 106(17):7131–7136, 2009. doi: 10.1073/pnas.0902232106. URL <https://www.pnas.org/doi/abs/10.1073/pnas.0902232106>.
- Dinu Kaufmann, Sonali Parbhoo, Aleksander Wieczorek, Sebastian Keller, David Adametz, and Volker Roth. Bayesian markov blanket estimation, 2015.
- Amelia Compagni, Petra Wilgenbus, Maria-Antonietta Impagnatiello, Matt Cotten, and Gerhard Christofori. Fibroblast Growth Factors Are Required for Efficient Tumor Angiogenesis1. *Cancer Research*, 60(24):7163–7169, 12 2000. ISSN 0008-5472.
- Ming Min Chang, Meng Shao Lai, Siou Ying Hong, Bo Syong Pan, Hsin Huang, Shang Hsun Yang, Chia Ching Wu, H. Sunny Sun, Jih Ing Chuang, Chia Yih Wang, and Bu Miin Huang. Fgf9/fgfr2 increase cell proliferation by activating erk1/2, rb/e2f1, and cell cycle pathways in mouse leydig tumor cells. *Cancer Science*, 109(11):3503–3518, November 2018. ISSN 1347-9032. doi: 10.1111/cas.13793.
- Waisberg J, De Souza Viana L, Affonso Junior RJ, Silva SR, Denadai MV, Margeotto FB, De Souza CS, and Matos D. Overexpression of the itgav gene is associated with progression and spread of colorectal cancer. *Anticancer Research*, 34(10):5599–5607, 2014. ISSN 0250-7005. URL <https://ar.iiajournals.org/content/34/10/5599>.
- Durk P Kingma, Tim Salimans, Rafal Jozefowicz, Xi Chen, Ilya Sutskever, and Max Welling. Improved variational inference with inverse autoregressive flow. In D. Lee, M. Sugiyama, U. Luxburg, I. Guyon, and R. Garnett, editors, *Advances in Neural Information Processing Systems*, volume 29. Curran Associates, Inc., 2016. URL https://proceedings.neurips.cc/paper_files/paper/2016/file/ddeebdeefdb7e7e7a697e1c3e3d8ef54-Paper.pdf.
- George Papamakarios, Theo Pavlakou, and Iain Murray. Masked autoregressive flow for density estimation, 2018.
- Fabricio Arend Torres. Sampling and annealing for dependency subnetwork estimation. Master’s thesis, University of Basel, 2018.

A Appendix

A.1 Sum-of-Sigmoids layers

We implement the proposed model with a conditional flow architecture that relies on element-wise transformations through monotonic functions, which we term Sum-of-Sigmoids. We further combine these element-wise monotonic transformations in an autoregressive fashion using a MADE-like approach [Kingma et al., 2016, Huang et al., 2018]. The proposed layers are light and very flexible and work particularly well for our purposes already with only 4 layers. Note that, even though it is not needed in our framework, the inverse can be computed numerically, which is relatively cheap since the transformation is element-wise monotonic. Specifically, we implement flexible monotonic transformations by combining shifted and scaled sigmoid activations. Differently from Huang et al. [2018], we also add shifted (and flipped) softplus functions to the element-wise activations. This leads to a linear behaviour outside a specific range $[-s, s]$, $s > 0$, alleviating the effect of inputs that lie outside the seen training data. The strictly monotonic element-wise transformation is given by

$$\phi_{sos}(z^{(i)}) = \underbrace{\left[a \sum_{j=1}^k v_j \sigma(w_j z^{(i)} + b_j) \right]}_{\text{sum of monotonic functions}} + \underbrace{\left[\ln \left(1 + e^{(z^{(i)}-s)} \right) - \ln \left(1 + e^{-(z^{(i)}-s)} \right) \right]}_{\text{approx. linear for } |z^{(i)}| \gg s, \text{ and zero for } |z^{(i)}| \ll s}, \quad (13)$$

where σ is the sigmoid function and $\{v_j, w_j, b_j\}_{j=1}^k$ and a are learnable parameters such that $w_k, v_j, a > 0$ and $\sum_{j=1}^k v_j = 1$. The advantage of using an element-wise transformation is that the associated Jacobian is diagonal and therefore its log-determinant is straightforward to compute. The proposed Sum-of-Sigmoids layers provide a very flexible transformation, but due to the element-wise nature, different dimensions are not mixed together. We overcome this by predicting the parameters $\{v_j, w_j, b_j\}_{j=1}^k$ and a of the Sum-of-Sigmoids with masked autoregressive hypernetworks, similar to other masked autoregressive flows. When implemented through masking Papamakarios et al. [2018], autoregressive flow allow for an elegant extension to conditional settings as well. Relevantly, this autoregressive structure admits a simple log-determinant Jacobian since the Jacobian is lower-triangular by construction.

A.2 Joint posterior for Ω_{11} and Ω_{12}

We show that given the partition in Eq. (12) and the prior in Eq. (7), the joint posterior factorizes as

$$p(\Omega_{11}, \Omega_{12}, \Omega_{22.1} | \mathcal{S}, \lambda, p) = p(\Omega_{11}, \Omega_{12} | \mathcal{S}, \lambda, p) p(\Omega_{22.1} | \mathcal{S}, \lambda, p). \quad (14)$$

We further provide the analytic expression for $p(\Omega_{11}, \Omega_{12} | \mathcal{S}, \lambda, p)$. The latter is used as target distribution in the training loss in Eq. (8) for the real data application in Section 4. For this proof we followed the approach of Torres [2018].

Let $\mathbf{X} \in \mathbb{R}^{n \times (s+t)}$ be the design matrix containing independent observations. We are interested in estimating the connections between s query variables with respect to the t remaining ones, typically with $s \ll t$. Given the partition of Ω and \mathcal{S} in Eq. (12), we define the full posterior $p(\Omega, \mathcal{S} | \lambda, p) = p(\Omega_{11}, \Omega_{12}, \Omega_{22}, \mathcal{S} | \lambda, p)$ as the product of the Wishart likelihood $p(\mathcal{S} | \Omega)$ and a suitable prior $p(\Omega | \lambda, p)$:

$$\begin{aligned} p(\mathcal{S} | \Omega) &\propto \mathcal{W}_{s+t}(n, \Omega^{-1}) = \det(\Omega)^{n/2} \exp\{\text{Tr}(-\frac{1}{2}\Omega\mathcal{S})\} \\ p(\Omega | \lambda, p) &\propto \mathcal{W}_{s+t}(s+t+1, \lambda \mathbf{1}_{s+t}) p(\Omega_{11} | \lambda, p) p(\Omega_{12} | \lambda, p). \end{aligned} \quad (15)$$

Specifically, we select a Wishart prior on Ω to ensure positive definiteness on the full matrix. In order to encourage sparsity we choose a generalized Normal distribution prior over the off-diagonal elements of Ω_{11} and over the full Ω_{12} :

$$p(\Omega_{11} | \lambda, p) \propto \prod_{i < j} \exp(-\lambda^p |(\Omega_{11})_{ij}|^p) \quad p(\Omega_{12} | \lambda, p) \propto \prod_{i, j} \exp(-\lambda^p |(\Omega_{12})_{ij}|^p). \quad (16)$$

As a first step we explicitly write down the expression for the likelihood

$$\begin{aligned} p(\mathcal{S} | \Omega) &= p(\mathcal{S} | \Omega_{11}, \Omega_{12}, \Omega_{22.1}) \\ &= \mathcal{W}_{s+t}(n, \Omega^{-1}) \\ &\propto \det(\Omega)^{n/2} \det(\mathcal{S})^{(n-(s+t)-1)/2} \exp(-\frac{1}{2}\text{Tr}[\Omega\mathcal{S}]) \end{aligned} \quad (17)$$

and for the prior

$$\begin{aligned}
p(\boldsymbol{\Omega}|\lambda, p) &= p(\boldsymbol{\Omega}_{11}, \boldsymbol{\Omega}_{12}, \boldsymbol{\Omega}_{22.1}|\lambda, p) \\
&\propto \mathcal{W}_{s+t}(s+t+1, \lambda \mathbf{1}_{s+t}) p(\boldsymbol{\Omega}_{11}|\lambda) p(\boldsymbol{\Omega}_{12}|\lambda) \\
&= \exp\left(-\frac{\lambda}{2} \text{Tr}[\boldsymbol{\Omega}]\right) \prod_{i<j} \exp\left(-\lambda^p |(\boldsymbol{\Omega}_{11})_{ij}|^p\right) \prod_{i,j} \exp\left(-\lambda^p |(\boldsymbol{\Omega}_{12})_{ij}|^p\right).
\end{aligned} \tag{18}$$

Overall, the posterior reads as

$$\begin{aligned}
p(\boldsymbol{\Omega}_{11}, \boldsymbol{\Omega}_{12}, \boldsymbol{\Omega}_{22.1}, \boldsymbol{S}|\lambda, p) &\propto \det(\boldsymbol{\Omega})^{n/2} \det(\boldsymbol{S})^{(n-(s+t)-1)/2} \\
&\times \exp\left(-\frac{1}{2} \text{Tr}[\boldsymbol{\Omega} \boldsymbol{S} + \lambda \boldsymbol{\Omega}]\right) \\
&\times \prod_{i<j} \exp\left(-\lambda^p |(\boldsymbol{\Omega}_{11})_{ij}|^p\right) \prod_{i,j} \exp\left(-\lambda^p |(\boldsymbol{\Omega}_{12})_{ij}|^p\right).
\end{aligned} \tag{19}$$

Following Kaufmann et al. [2015], we now re-write the posterior through the change of variables $(\boldsymbol{\Omega}_{11}, \boldsymbol{\Omega}_{12}, \boldsymbol{\Omega}_{22}) \rightarrow (\boldsymbol{\Omega}_{11}, \boldsymbol{\Omega}_{12}, \boldsymbol{\Omega}_{22.1})$ involving the Schur component $\boldsymbol{\Omega}_{22.1} = \boldsymbol{\Omega}_{22} - \boldsymbol{\Omega}_{12}^T \boldsymbol{\Omega}_{11}^{-1} \boldsymbol{\Omega}_{12}$. Note that the transformation has unit Jacobian: $J((\boldsymbol{\Omega}_{11}, \boldsymbol{\Omega}_{12}, \boldsymbol{\Omega}_{22}) \rightarrow (\boldsymbol{\Omega}_{11}, \boldsymbol{\Omega}_{12}, \boldsymbol{\Omega}_{22.1})) = \mathbf{1}$. We can now explicitly re-write the posterior as $p(\boldsymbol{\Omega}_{11}, \boldsymbol{\Omega}_{12}, \boldsymbol{\Omega}_{22.1}, \boldsymbol{S}|\lambda, p)$ by using the following substitutions, which are straightforward to show:

$$\begin{aligned}
\det(\boldsymbol{\Omega}) &= \det(\boldsymbol{\Omega}_{11}) \det(\boldsymbol{\Omega}_{22} - \boldsymbol{\Omega}_{12}^T \boldsymbol{\Omega}_{11}^{-1} \boldsymbol{\Omega}_{12}) = \det(\boldsymbol{\Omega}_{11}) \det(\boldsymbol{\Omega}_{22.1}), \\
\text{Tr}(\boldsymbol{\Omega} \boldsymbol{S}) &= \text{Tr}[\boldsymbol{\Omega}_{11} \boldsymbol{S}_{11} + \boldsymbol{\Omega}_{12} \boldsymbol{S}_{12}^T + \boldsymbol{\Omega}_{12}^T \boldsymbol{S}_{12} + \boldsymbol{\Omega}_{22.1} \boldsymbol{S}_{22} + \boldsymbol{\Omega}_{12}^T \boldsymbol{\Omega}_{11}^{-1} \boldsymbol{\Omega}_{12} \boldsymbol{S}_{22}], \\
\text{Tr}(\lambda \boldsymbol{\Omega}) &= \text{Tr}[\lambda \boldsymbol{\Omega}_{11} + \lambda \boldsymbol{\Omega}_{22.1} + \lambda \boldsymbol{\Omega}_{12}^T \boldsymbol{\Omega}_{11}^{-1} \boldsymbol{\Omega}_{12}].
\end{aligned} \tag{20}$$

By re-arranging the terms the posterior simplifies to:

$$\begin{aligned}
p(\boldsymbol{\Omega}_{11}, \boldsymbol{\Omega}_{12}, \boldsymbol{\Omega}_{22.1}, \boldsymbol{S}|\lambda, p) &\propto \det(\boldsymbol{\Omega}_{11})^{n/2} \det(\boldsymbol{S})^{\frac{n-(s+t)-1}{2}} \\
&\times \det(\boldsymbol{\Omega}_{22.1})^{n/2} \exp\left(-\frac{1}{2} \text{Tr}[\boldsymbol{\Omega}_{22.1}(\boldsymbol{S}_{22} + \lambda \mathbf{1}_t)]\right) \\
&\times \exp\left(-\frac{1}{2} \text{Tr}[\boldsymbol{\Omega}_{11}(\boldsymbol{S}_{11} + \lambda \mathbf{1}_s) + 2(\boldsymbol{\Omega}_{12}^T \boldsymbol{S}_{12}) + \boldsymbol{\Omega}_{12}^T \boldsymbol{\Omega}_{11}^{-1} \boldsymbol{\Omega}_{12}(\boldsymbol{S}_{22} + \lambda \mathbf{1}_t)]\right) \\
&\times \prod_{i<j} \exp\left(-\lambda^p |(\boldsymbol{\Omega}_{11})_{ij}|^p\right) \prod_{i,j} \exp\left(-\lambda^p |(\boldsymbol{\Omega}_{12})_{ij}|^p\right).
\end{aligned}$$

If we now condition on \boldsymbol{S} , and specifically on \boldsymbol{S}_{22} , we can clearly see that the posterior factorizes as $p(\boldsymbol{\Omega}_{11}, \boldsymbol{\Omega}_{12}, \boldsymbol{\Omega}_{22.1}|\boldsymbol{S}, \lambda, p) \propto p(\boldsymbol{\Omega}_{11}, \boldsymbol{\Omega}_{12}|\boldsymbol{S}, \lambda, p) p(\boldsymbol{\Omega}_{22.1}|\boldsymbol{S}, \lambda, p)$. In particular, we are interested in estimating the joint posterior $p(\boldsymbol{\Omega}_{11}, \boldsymbol{\Omega}_{12}|\boldsymbol{S}, \lambda, p)$, which reads as

$$\begin{aligned}
p(\boldsymbol{\Omega}_{11}, \boldsymbol{\Omega}_{12}|\boldsymbol{S}, \lambda, p) &\propto \det(\boldsymbol{\Omega}_{11})^{n/2} \\
&\times \exp\left(-\frac{1}{2} \text{Tr}[\boldsymbol{\Omega}_{11}(\boldsymbol{S}_{11} + \lambda \mathbf{1}_s) + 2(\boldsymbol{\Omega}_{12}^T \boldsymbol{S}_{12}) + \boldsymbol{\Omega}_{12}^T \boldsymbol{\Omega}_{11}^{-1} \boldsymbol{\Omega}_{12}(\boldsymbol{S}_{22} + \lambda \mathbf{1}_t)]\right) \\
&\times \prod_{i<j} \exp\left(-\lambda^p |(\boldsymbol{\Omega}_{11})_{ij}|^p\right) \prod_{i,j} \exp\left(-\lambda^p |(\boldsymbol{\Omega}_{12})_{ij}|^p\right)
\end{aligned}$$

A.3 Run-time comparison with Gibbs sampler

The proposed Conditional Matrix Flow provides a significant speed-up with respect to standard Gibbs sampling algorithms for posterior inference in Gaussian Graphical Models. Most importantly, we leverage GPUs for an enormous speed-up during training. In contrast, individual chains sampled with MCMC can only gain a comparatively limited speed-up on the GPU due to the sequential nature of the method.

For a realistic and fair comparison, we measure run-time on our real data experiment. For this purpose, we trained the Conditional Matrix Flow for $p = 1$ and compare it against the Gibbs sampler introduced in Kaufmann et al. [2015]. The setting presented here is the same one used to obtain the results shown in the Experiment section. The Gibbs sampler takes 89 seconds to generate 500 samples, which translates to about 5.6 samples per second. This result was obtained on a Intel(R)

Xeon(R) CPU E5-1660 v3 @ 3.00GHz. We train the Conditional Matrix Flow from $T_0 = 5$ to $T_n = 1$ for 400 epochs with the geometric cooling schedule $T_i = T_0 a^i$ for $a = T_n/T_0$. On the consumer-grade GPU NVIDIA TITAN X (12GB VRAM) training takes less than 3 minutes and sampling is extremely efficient: each second we can generate 2000 independent samples from the approximate posterior. Taking training time into account for the conditional flow and a burn-in period for the Gibbs sampler, the proposed method is three orders of magnitude faster than the Gibbs sampler. When sampling for different λ values, the difference becomes even more pronounced because different λ require independent Markov Chains. In contrast, with the proposed framework we can draw independent samples for different λ values at the same computational cost.

A.4 Artificial data: MAP estimate for different sub- l_1 pseudo-norms

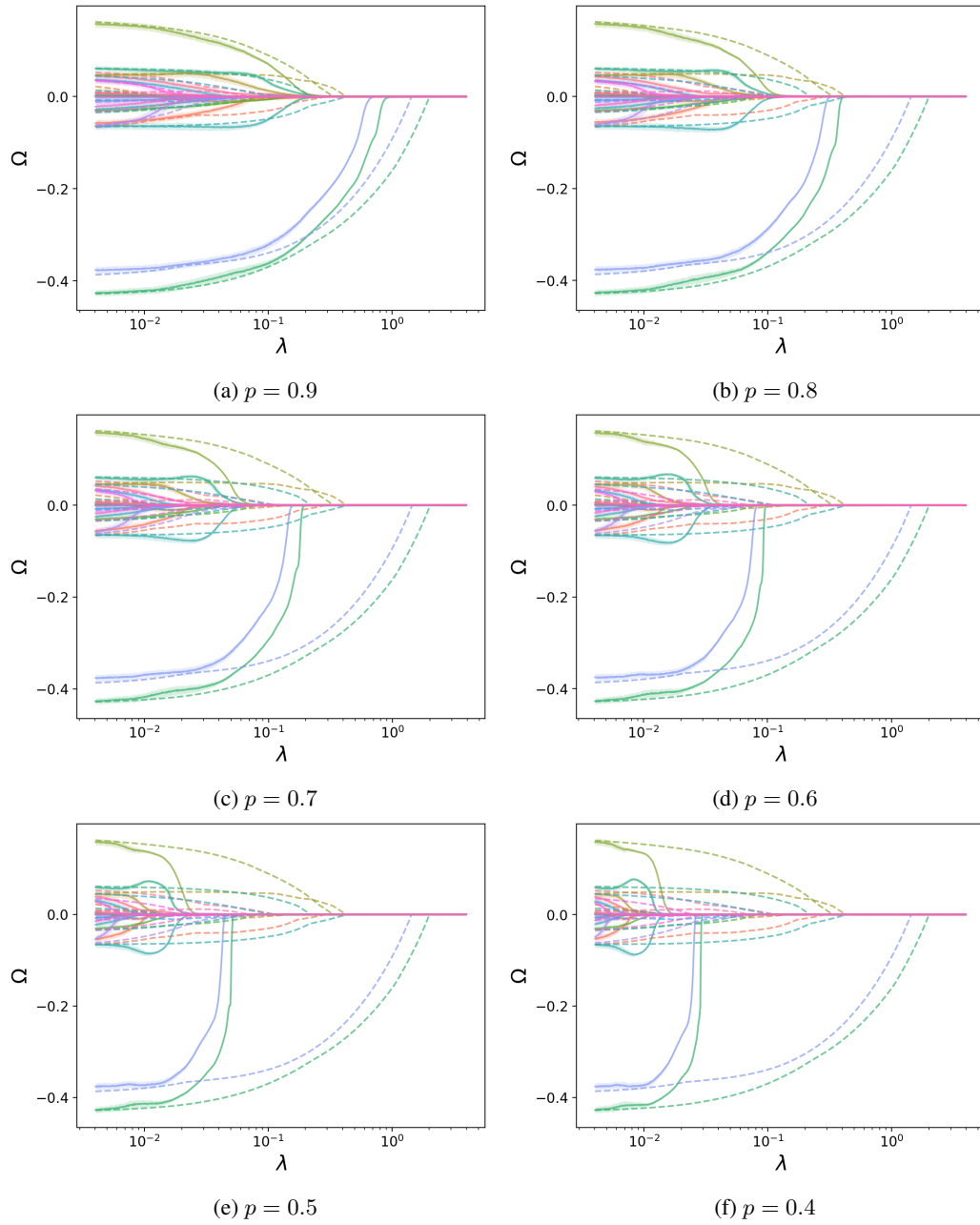


Figure 5: MAP estimate as a function of λ for different sub- l_1 pseudo-norms. The dashed line is the frequentist solution path for $p = 1$.